Collapse of odd-integer Hall gaps in double quantum wells due to edge effects

O. G. Balev
Departamento de Física, Universidade Federal de São Carlos, 13565-905, São Carlos, São Paulo, Brazil and Institute of Semiconductor Physics, National Academy of Sciences, 45 Pr. Nauky, Kiev 252650, Ukraine

Nelson Studart
Departamento de Física, Universidade Federal de São Carlos, 13565-905, São Carlos, São Paulo, Brazil
(Received 23 May 2002; revised manuscript received 4 February 2003; published 8 April 2003)

We show, within the Hartree-Fock approximation, that the quantum Hall effect for total filling factor $\nu = 1, 3, 5,$ and 7 can be destroyed due to many-body effects induced by the edges of a bilayer system. For $\nu = 1$, we also study the correlation effects, in addition to the exchange interaction, which are mainly related to the edge-state screening. Calculation results explain quite well the experimental behavior observed in double-quantum-well structures with rather large tunnel splitting $\Delta_{SAS} \gtrsim 0.5$ K.

DOI: 10.1103/PhysRevB.67.155305 PACS number(s): 73.43.−f, 73.21.Fg

I. INTRODUCTION

The quantum Hall effect (QHE) in bilayer systems, especially in double-quantum-well (DQW) structures, has attracted great attention because remarkable new quantum phenomena have been discovered.[1] In symmetric DQW's besides the Coulomb interaction between electrons in different quantum wells, there is a new energy scale associated to the symmetric-antisymmetric (SAS) energy gap Δ_{SAS} due to interwell tunneling. If Δ_{SAS} is much larger than the thermal energy, new steps in the Hall conductance are expected to appear at the odd total filling factor ν in the absence of Coulombic effects. However, magnetotransport measurements show the collapse of integer QHE's associated with the SAS gap at large well separations.[2–5] Theoretical investigations for $\nu = 1$[6–8] and $\nu = 3, 5, 7$ (Ref. 6) predict that interaction effects may destroy this gap because the charge-density excitation spectrum develops a soft mode when the well separation is on the order of the magnetic length. In particular, for $\nu = 1$ the combined effect of single-particle tunneling and many-body interactions can enhance as well as destroy the QHE, and quantum phase transitions should be created from a regime dominated by inter-well tunneling into one where highly correlated liquids and Wigner crystals can be developed.[1,5,9,10] To our best knowledge, theoretical calculations for the collapse of odd integer Hall gaps in a DQW system are fully ''bulklike'' in the sense that effects coming from edge states[11] are completely ignored.

In this paper, we investigate the edge-state effects on the collapse of the odd integer Hall effect in the DQW systems. Firstly, we show that even in the Hartree-Fock approximation (HFA) that does not include electron correlations, the combined effect of the lateral confinement and the exchange interaction may lead to the collapse of the $\nu = 1, 3, 5, 7$ Hall gaps in DQW's, i.e., the edge states due to the lateral confinement induce drastic changes in the bulklike properties of the whole wide DQW channel. The present calculation describes quite well the experimental results for all three samples of the seminal work[2] for the $\nu = 1, 3, 5, 7$ QHE regime, going beyond the results of the single-mode-approximation calculations.[6] Secondly, we take into account the influence of strong correlations, induced by the edge states, on the collapse of the $\nu = 1$ Hall gap in the DQW by using a generalized local-density approximation (GLDA).[12] In addition, for $\nu = 1$ we show that correlations, coming from, which we call a quasiresonance screening, which is essential, in particular, when the cyclotron frequency $\omega_c \gg \Delta_{SAS}/\hbar$, in the inner part of the DQW channel, contribute to inhibit the Hall gap collapse. However, the latter effect is typically much weaker than the effect of correlations related with the edge-state screening. We show that particle correlations do not restore the $\nu = 1$ Hall gap when it was already collapsed within the HFA. Furthermore, correlations can lead to the collapse of Hall gaps unpredictable within the HFA.

We extend the GLDA for a realistic DQW model (finite thickness of barriers and wells, the interwell tunneling, etc.) to treat in a self-consistent way the effect of correlations induced by the edge-state screening. We calculate the group velocity of the edge states renormalized by exchange and correlations. We make a detailed comparison with the experimental results of the seminal works of Refs. 2 and 5. We find a good agreement with our calculation results.

The paper is organized as follows. In Sec. II we present the one-electron spectrum of the Landau levels of a DQW channel. In Sec. III we study the destruction of the QHE states showing that exchange effects from the edges of a DQW can lead to the collapse of $\nu = 1, 3, 5,$ and 7 Hall gaps and the experimental results of Ref. 2 are analyzed within the HFA. In Sec. IV the exchange-correlation effects at the edge and at the bulk of symmetric DQW's, on the $\nu = 1$ Hall gap are studied and the possibility of the destruction of the $\nu = 1$ QHE state due to correlations is investigated. In Sec. V we summarize our results.

II. DQW CHANNEL IN A STRONG MAGNETIC FIELD

We consider a two-dimensional (2D) electron system (2DES) in the presence of a strong magnetic field B along the perpendicular direction (z axis) confined in a DQW channel of width W and length $L_x = L$. We treat the electrons in the effective-mass approximation characterized by an effective mass m^* moving in a medium with a dielectric constant ϵ

that is assumed constant across the DQW structure. It consists of two finite square wells (depth U) along the z axis, with widths d_l and d_r, and separated by a potential barrier of width d_b. In the model the interwell tunneling is implicitly included by considering two closely located levels due to the ground levels of the left (l) and right (r) isolated QW's. For weak barrier penetration, the DQW wave functions can be written as[13,14]

$$\zeta_-(z)=N\{X_r(z)-[2T/(\Delta+\Delta_T)]X_l(z)\},$$

$$\zeta_+(z)=N\{X_l(z)+[2T/(\Delta+\Delta_T)]X_r(z)\}, \quad (1)$$

where the normalization factor $N=\sqrt{(\Delta+\Delta_T)/2\Delta_T}$. The energy gap $\Delta_T=\sqrt{\Delta^2+4T^2}$, where Δ is the energy splitting of the isolated l and r levels and the tunneling matrix element $T=-T_0\exp(-\kappa d_b)$ $(T_0\approx 2\pi^2\hbar^2/m^*\kappa d_l^{3/2}d_r^{3/2})$ with $\kappa^{-1}\approx\hbar/\sqrt{2m^*U}$. For the most studied symmetric DQW's, $\Delta=0$, $\Delta_T=\Delta_{\rm SAS}=\varepsilon_a-\varepsilon_s$ is the SAS gap in the one-electron approximation and $\zeta_{-,+}(z)=\zeta_{s,a}(z)$ are the symmetric and antisymmetric wave functions.

We consider a lateral confinement model described by a symmetric potential given by $V_y=0$ in the inner part of the channel and $V_y=m^*\Omega^2(y-y_r)^2/2$, $y\geqslant y_r$ at the right edge. V_y is assumed to be smooth on the scale of $\ell_0=(\hbar/m^*\omega_c)^{1/2}$ such that $\Omega\ll\omega_c$, where $\omega_c=|e|B/m^*c$ is the cyclotron frequency. Choosing the Landau gauge, $\mathbf{A}=(-By,\ 0,\ 0)$, the electron wave function in the plane is given by $\Psi_{n,k_x}(x,y)\phi_\sigma=e^{ik_xx}\psi_n(y-y_0)\phi_\sigma/\sqrt{L}$, where ϕ_σ represents spin states for spin up ($\uparrow$) and down ($\downarrow$) of the z component of the spin operator with eigenvalues $\sigma=1$ and $\sigma=-1$, $\psi_n(y)$ is a harmonic oscillator function and $y_0\equiv y_0(k_x)=\ell_0^2k_x$. The energy eigenvalues for the bulk or right-edge region of the channel, are well approximated by[14]

$$\varepsilon_{n,\sigma}(k_x)=(n+\tfrac{1}{2})\hbar\omega_c+\tfrac{1}{2}[m^*\Omega^2(y_0-y_r)^2\Theta(y_0-y_r)+\sigma g_0\mu_BB], \quad (2)$$

where $\Theta(x)$ is the step function, $g_0(<0)$ is the bare Landé g factor, μ_B is the Bohr magneton, and $y_r=k_r\ell_0^2$. Summarizing the results, the total electron wave function is given by $\Psi_{n,k_x,\sigma,i}(x,y)=\Psi_{n,k_x}(x,y)\phi_\sigma\zeta_i(z)$, where i stands for levels $(-,+)$, with the corresponding energies $\varepsilon_{n,\sigma,i}(k_x)=\varepsilon_{n,\sigma}(k_x)+\varepsilon_i$, where $\varepsilon_\pm=\pm\Delta_T/2$.

Throughout the paper, if otherwise is not stated, we will consider $\nu=1$ and assume that all the electrons are in the lowest Landau sublevel (LSL) ($n=0$, $\sigma=1$, $i=-$). Then in the independent-particle model (Hartree approximation), the total energy spectrum in the bulk or in the right-edge region of the DQW channel for the four lowest LSL's is given as

$$\varepsilon_{0,\sigma,\pm}(k_x)=[\hbar\omega_c+m^*\Omega^2(y_0-y_r)^2\Theta(y_0-y_r)-\sigma|g_0|\mu_BB\pm\Delta_T]/2. \quad (3)$$

From Eq. (3) we define the group velocity of the LSL edge states as $v_{g0,1}^{-,H}=\hbar^{-1}[\partial\varepsilon_{0,1,-}(k_r+k_{e,1}^{0,-})/\partial k_x]=\hbar\Omega^2k_{e,1}^{0,-}/m^*\omega_c^2$ with $k_{e,1}^{0,-}=(\omega_c/\hbar\Omega)\sqrt{2m^*\Delta_{F0,1}^-}$, where $\Delta_{F0,1}^-=E_F^H-[\hbar\omega_c-|g_0|\mu_BB-\Delta_T]/2>0$, and E_F^H is the Fermi energy; superscript H stands for the Hartree approximation. The edge of the LSL is denoted by $y_{r0,1}^-=\ell_0^2k_{r,1}^{0,-}$, where $k_{r,1}^{0,-}=k_r+k_{e,1}^{0,-}$, and $W=2y_{r0,1}^-$. Similar characteristic wave vectors $k_{e,\sigma}^{n,i}$ can be written for $\nu=3,5,7$. We assume that $W\gg\ell_0$ such that when many-body interactions are taken into account, the energy spectrum at the right edge of the DQW is totally independent of the left edge. In particular, $\tilde{k}_{r,1}^{0,-}=k_{r,1}^{0,-}\ell_0\gg 1$ and we will use notation $\tilde{k}_x=k_x\ell_0$.

III. COLLAPSE OF ODD QHE STATES IN THE DQW DUE TO EXCHANGE EFFECTS AT THE EDGES

It is well known that we can obtain exchange and correlations contributions for the self-energy of an interacting system by considering the exchange contribution to first order of $r_0=e^2/\epsilon\ell_0\hbar\omega_c$ in the screened Hartree-Fock approximation.[15] In the DQW channel, the electron self-energy takes the form[12]

$$E_{0,k_x,\sigma,i}=\varepsilon_{0,\sigma,i}(k_x)+\varepsilon_{0,k_x,\sigma,i}^{xc}, \quad (4)$$

where (for $\nu=1,3$)

$$\varepsilon_{0,k_x,\sigma,i}^{xc}=-\frac{1}{(2\pi)^3}\sum_{j>0}^{\pm}\int_{-k_{r,\sigma}^{0,j}}^{k_{r,\sigma}^{0,j}}dk_x'\int_{-\infty}^{\infty}\cdots\times\int_{-\infty}^{\infty}dq_ydq_y'dzdz'\zeta_i(z)\zeta_j(z)\zeta_j(z')\zeta_i(z')\times V^s(k_-;q_y,q_y';z,z')(0k_x|e^{iq_yy}|0k_x')\times(0k_x'|e^{iq_y'y'}|0k_x), \quad (5)$$

and $V^s(q_x;q_y,q_y';z,z')$ is the 2D Fourier transform of the screened Coulomb interaction, $k_\pm=k_x\pm k_x'$ and the matrix element $(0k_x|e^{iq_yy}|0k_x')=\exp\{-[k_-^2+q_y^2-2iq_yk_x]\ell_0^2/4\}$. The summation over j includes only occupied LSL's. If neglect by screening in $V^s(q_x;q_y,q_y';z,z')$, substituting the bare electron-electron interaction

$$V_{\rm bare}(q_x;q_y,q_y';z,z')=\frac{4\pi^2e^2}{\epsilon q}\delta(q_y+q_y')e^{-q|z-z'|} \quad (6)$$

into Eq. (5), we obtain the exchange contribution $\varepsilon_{0,k_x,1,i}^x$ which, in the regions far from the edges of the DQW channel, reproduces the exact HFA result for the energy in the "bulk" model. In our calculations we take in Eq. (1) the approximated form $X_{l,r}(z)=\sqrt{2/d_{l,r}}\cos[\pi(z-z_{l,r})/d_{l,r}]$ for $|z-z_{l,r}|\leqslant d_{l,r}/2$, and zero for $|z-z_{l,r}|\geqslant d_{l,r}/2$, where z_l and z_r are the centers of l and r QW's, respectively. We denote $d\equiv z_r-z_l=d_b+(d_l+d_r)/2$.

Now we describe the exchange renormalization of the LSL's and the pinning of the Fermi level due to edge effects. First, we consider $\nu=1$. Substituting Eq. (6) into Eq. (5), we obtain the exchange contribution to the single-particle energy in the form

$$\varepsilon^{x}_{0,k_x',1,i}=-\frac{e^2}{2\pi\epsilon}\int_{-k^{0,-}_{r,1}}^{k^{0,-}_{r,1}}dk_x'\int_{-\infty}^{\infty}dq_y\frac{e^{-(k_-^2+q_y^2)\ell_0^2/2}}{\sqrt{k_-^2+q_y^2}}\int dz \times\int dz' e^{-|z-z'|\sqrt{k_-^2+q_y^2}}\zeta_i(z)\zeta_-(z')\zeta_i(z')\zeta_-(z). \tag{7}$$

For $d_{l,r}\to 0$ and $\tilde{k}^{-}_{r0,1}-|\tilde{k}_x|\gg 1$, it follows that

$$\varepsilon^{x(\nu=1)}_{0,1,-}=-\sqrt{\frac{\pi}{2}}\frac{e^2}{\epsilon\ell_0}\left[\frac{\Delta^2+2T^2}{\Delta^2+4T^2}+\frac{2T^2}{\Delta^2+4T^2}e^{d^2/2\ell_0^2}\mathrm{erfc}\left(\frac{d}{\sqrt{2}\ell_0}\right)\right], \tag{8}$$

and

$$\varepsilon^{x(\nu=1)}_{0,1,+}=-\sqrt{\frac{\pi}{2}}\frac{e^2}{\epsilon\ell_0}\frac{2T^2}{\Delta^2+4T^2}\left[1-e^{d^2/2\ell_0^2}\mathrm{erfc}\left(\frac{d}{\sqrt{2}\ell_0}\right)\right], \tag{9}$$

where $\mathrm{erfc}(x)$ is the complementary error function. Thus, the exchange-enhanced splitting between $(n=0,\ \sigma=1,\ i=\pm)$ the LSL's is given as

$$\varepsilon^{x(\nu=1)}_{0,1,+}-\varepsilon^{x(\nu=1)}_{0,1,-}=\frac{e^2}{\epsilon\ell_0}\sqrt{\frac{\pi}{2}}\left[\frac{\Delta^2}{\Delta^2+4T^2}+\frac{4T^2}{\Delta^2+4T^2}e^{d^2/2\ell_0^2}\mathrm{erfc}\left(\frac{d}{\sqrt{2}\ell_0}\right)\right]. \tag{10}$$

For a symmetric DQW system, $\Delta=0$, Eq. (10) gives $(e^2/\epsilon\ell_0)\sqrt{\pi/2}\exp(d^2/2\ell_0^2)\mathrm{erfc}(d/\sqrt{2}\ell_0)$, which is independent of the tunneling matrix element T and tends to $\sqrt{\pi/2}(e^2/\epsilon\ell_0)$, for $d/\ell_0\ll 1$, or to $(e^2/\epsilon d)$, for $(d/\ell_0)^2\gg 1$. Then for $\nu=1$ and $\Delta=0$ the exchange-enhanced splitting of the lowest $i=\pm$ LSL's, in the bulk of the DQW channel, is substantially greater than $\Delta_{\mathrm{SAS}}=2|T|$ or the usual Zeeman spin splitting $|g_0|\mu_B B$. Notice that, for $\Delta^2\gg 4T^2$, the enhanced splitting $\sqrt{\pi/2}(e^2/\epsilon\ell_0)$ coincides with the exchange enhancement of "regular" spin splitting.[15]

Furthermore, at the DQW edge we obtain, from Eq. (7), that $\varepsilon^{x}_{0,\pm k^{0,-}_{r,1},1,-}=\varepsilon^{x(\nu=1)}_{0,1,-}/2$. At the LSL edge, $k_x=\pm k^{0,-}_{r,1}$, the exchange energy of the $(i=-)$ LSL is two times smaller than that for the inner part of the DQW channel. Then the Fermi level pinning due to the exchange effects at the edges is given by

$$E_F=\tfrac{1}{2}[\hbar\omega_c+m^*\Omega^2\ell_0^4(k^{0,-}_{e,1})^2-|g_0|\mu_B B-\Delta_T+\varepsilon^{x(\nu=1)}_{0,1,-}]. \tag{11}$$

For $(\tilde{k}^{-}_{r0,1}-|\tilde{k}_x|)\gg 1$, the energy of the bottom of the empty $(n=0,\ \sigma=1,\ i=+)$ LSL is given as

$$E_{0,1,+}=\tfrac{1}{2}[\hbar\omega_c-|g_0|\mu_B B+\Delta_T]+\varepsilon^{x(\nu=1)}_{0,1,+}, \tag{12}$$

where $\varepsilon^{x(\nu=1)}_{0,1,+}$ is defined by Eq. (9).

The $\nu=1$ Hall gap is then written as

$$E_{0,1,+}-E_F=\sqrt{\Delta^2+4T^2}-\frac{m^*\Omega^2}{2}\ell_0^4(k^{0,-}_{e,1})^2-\frac{1}{2}\sqrt{\frac{\pi}{2}}\frac{e^2}{\epsilon\ell_0}\times\left[\frac{2T^2-\Delta^2}{\Delta^2+4T^2}-\frac{6T^2}{\Delta^2+4T^2}e^{d^2/2\ell_0^2}\mathrm{erfc}\left(\frac{d}{\sqrt{2}\ell_0}\right)\right]. \tag{13}$$

Notice that $(E_F-E_{0,1,-})$, in contrast with $(E_{0,1,+}-E_F)$, is always positive and rather large, of the order in $e^2/\epsilon\ell_0$. For symmetric DQW, $\Delta=0$ and $d_l=d_r$, Eq. (13) yields

$$E_{0,1,+}-E_F=2|T|-\frac{m^*\Omega^2}{2}\ell_0^4(k^{0,-}_{e,1})^2-\frac{1}{4}\sqrt{\frac{\pi}{2}}\frac{e^2}{\epsilon\ell_0}\left[1-3e^{d^2/2\ell_0^2}\mathrm{erfc}\left(\frac{d}{\sqrt{2}\ell_0}\right)\right]. \tag{14}$$

We observe in Eq. (14) that the collapse of the $\nu=1$ Hall gap occurs when d/ℓ_0 is sufficiently large such that $\exp(d^2/2\ell_0^2)\mathrm{erfc}(d/\sqrt{2}\ell_0)<1/3$ and

$$\frac{1}{4}\sqrt{\frac{\pi}{2}}\frac{e^2}{\epsilon\ell_0}\left[1-3e^{d^2/2\ell_0^2}\mathrm{erfc}\left(\frac{d}{\sqrt{2}\ell_0}\right)\right]\geqslant 2|T|. \tag{15}$$

For the interesting case of $|T|\to 0$, in the HFA there is a finite $\nu=1$ Hall gap when $d<\eta\ell_0$, while this gap is collapsed for $d\geqslant\eta\ell_0$, where $\eta\approx 2.023$ is the solution of the equation $3\exp(\eta^2/2)\mathrm{erfc}(\eta/\sqrt{2})-1=0$.

For the $\nu=3$ Hall gap $(E_{0,-1,+}-E_F)$ expressions are obtained from Eq. (13) or, for $\Delta=0$, Eq. (14) after changing $k^{0,-}_{e,1}$ by $k^{0,-}_{e,-1}$. The bottoms of the occupied LSL's are located at $[\hbar\omega_c-|g_0|\mu_B B\mp\Delta_T-\sqrt{2\pi}e^2/\epsilon\ell_0]/2$, for $(n=0,\ \sigma=1,\ i=\mp)$ LSL's and at $E_{0,-1,-}=(\hbar\omega_c+|g_0|\mu_B B-\Delta_T)/2+\varepsilon^{x(\nu=1)}_{0,1,-}$, for $(n=0,\ \sigma=-1,\ i=-)$ LSL. The bottom of the empty $(n=0,\ \sigma=-1,\ i=+)$ LSL is at $E_{0,-1,+}=(\hbar\omega_c+|g_0|\mu_B B+\Delta_T)/2+\varepsilon^{x(\nu=1)}_{0,1,+}$.

Further we present the results only for symmetric DQW's and we take the interwell spacing $d=d_l+d_b$ by the experimental values of d_l and d_b (Ref. 6). In Fig. 1 we depict the phase diagram of the collapse of the QHE in a DQW. The boundary depends on d/ℓ_0 and the Hartree gap $\Delta_H/(e^2/\varepsilon\ell_0)$. The heavy solid curve represents d/ℓ_0, for $\nu=1$, as a function of the Hartree gap $\Delta_H=\varepsilon_{0,1,+}(0)-E_F^H=2|T|-m^*\Omega^2\ell_0^4(k^{0,-}_{e,1})^2/2$, where $\varepsilon_{0,1,+}(0)$ is given by Eq. (3). d/ℓ_0 was calculated from Eq. (14) for $\Delta_x(v^{-,H}_{g0,1})=E_{0,1,+}-E_F=0$. This curve corresponds to a zero Hall gap within the HFA. For $\nu=3$, the same curve represents d/ℓ_0 as a function of the Hartree gap $\varepsilon_{0,-1,+}(0)-E_F^H=2|T|-m^*\Omega^2\ell_0^4(k^{0,-}_{e,-1})^2/2$, which corresponds to a zero Hall gap in the HFA for $\nu=3$. We can also rewrite the Hartree gap as $\Delta_H(v^{-,H}_{g0,\sigma})=2|T|-m_p(v^{-,H}_{g0,\sigma})^2/2$ where $m_p=m^*\omega_c^2/\Omega^2$ and $\sigma=1(-1)$ for $\nu=1(3)$. It is seen that if the condition $4|T|-m^*\Omega^2\ell_0^4(k^{0,-}_{e,\pm 1})^2<0$ is fulfilled, i.e., even when the Hartree-Hall gap is absent, the Hall gap can still exist within the HFA for $\nu=1,3$. The heavy solid curve delimits, for $d_l/d=0$, the region where the QHE states exist (below) and

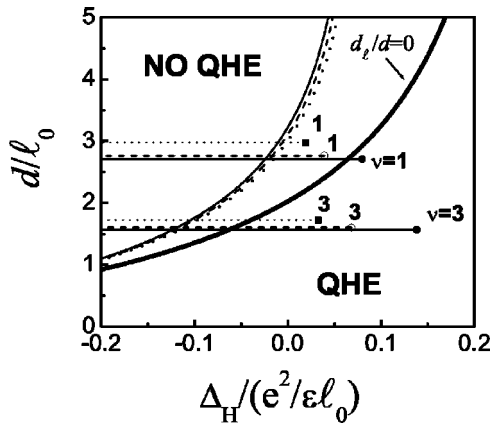

FIG. 1. Phase diagram for the $\nu=1,3$ QHE in a symmetric DQW, within the HFA. The heavy solid curve is the calculated phase boundary, for $d_l/d=0$, of the $n=0$ Landau level for collapse of the energy Hall gap. $\Delta_H(v_{g0,\sigma}^{-,H})$ is the energy gap between the bottom of the lowest unoccupied Landau sublevel and the Fermi level in the Hartree approximation, $d=d_b+d_l$ and $\ell_0=(\hbar c/eB)^{1/2}$. The experimental data for $\nu=1(3)$ from the three samples of Ref. 2 are represented by solid circle (a DQW with barrier thickness $d_b=28$ Å), open circle ($d_b=40$ Å), and solid square ($d_b=51$ Å). The solid, dashed, and dotted straight lines indicate the modification of the data positions as $v_{g0,\sigma}^{-,H}$ varies. The thin solid, dashed, and dotted curves include our finite-well-thickness corrections for $d_l/d=0.83(d_b=28$ Å), $0.78(d_b=40$ Å), and 0.73 ($d_b=51$ Å), respectively.

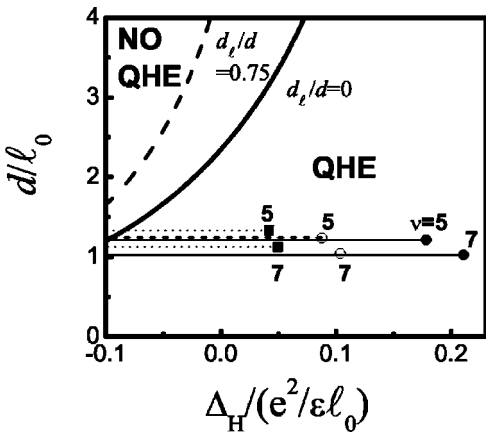

FIG. 2. Same as in Fig. 1, for the $n=1$ Landau level with data for $\nu=5,7$. The thin dashed curve represents the phase boundary for $d_l/d=0.75$.

the other one of missing QHE states (above) in which the Hall gap collapses because it becomes formally negative. Pairs of points indicated by solid circle, open circle and solid square in Fig. 1 correspond to samples data of Ref. 2 with $d_b=28$, 40, and 51 Å, respectively. At the maximum of the pertinent Hall gap, these marks correspond to $k_{e,1}^{0,-}=0$ for $\nu=1$, while they correspond to $k_{e,-1}^{0,-}=0$ for $\nu=3$. Starting from these marks, the solid, dashed, and dotted horizontal lines represent their changes when $k_{e,\pm1}^{0,-}\neq0$. Now we proceed to compare our results with the experimental data of Ref. 2. We conclude by using the $d_l=0$ approximation that (i) for $d_b=28$ Å both $\nu=1$ and $\nu=3$ QHE were observed according to our predictions; (ii) for $d_b=40$ Å only the $\nu=1$ Hall gap collapses (see that the dashed straight line lies totally within the no-QHE region) while the $\nu=3$ Hall gap may be present in agreement with the experimental results; (iii) for $d_b=51$ Å the $\nu=1$ QHE state is absent, as observed in the experiment, whereas the $\nu=3$ QHE state can exist, but was not observed experimentally. Then the HFA results for the collapse of $\nu=1,3$ Hall gaps are in good agreement with the experimental ones. It should be pointed out that our HFA calculation reproduces better the experimental achievements than that based on a single-mode approximation.[6]

In addition, we shortly discuss the changes in the phase boundary due to the finite width of the DQW. We represent in Fig. 1 the phase boundary by the solid, dashed, and dotted curves for $d_l/d=0.83$ ($d_b=28$ Å), $d_l/d=0.78$ ($d_b=40$ Å), and $d_l/d=0.73$ ($d_b=51$ Å), respectively. The influence of the finite width is to decrease the region for the QHE collapse. For instance, the $\nu=1$ and $\nu=3$ QHE states can be observed for the samples with $d_b=40$ and 51 Å.

Now we briefly discuss the possibility of the nonoccurrence of the $\nu=5,7$ QHE states within our HFA picture. For the symmetric DQW, with a finite d_l, a similar procedure as developed above leads to $\nu=5,7$ Hall energy gaps given by

$$E_{1,\pm1,+}-E_F=2|T|-\frac{m^*\Omega^2}{2}\ell_0^4(k_{e,\pm1}^{1,-})^2 - \frac{e^2}{\epsilon\ell_0}\int_0^\infty dq e^{-q^2/2}(1-q^2/2)^2 \times\int_{-1/2}^{1/2}dx\int_{-1/2}^{1/2}dx'\cos^2(\pi x)\cos^2(\pi x') \times\{e^{-q(d_l/\ell_0)|x-x'|}-3e^{-q|d_l(x-x')-d|/\ell_0}\}. \tag{16}$$

Equation (16) is obtained assuming that $\tilde{k}_{e,\pm1}^{1,-}-\tilde{k}_{e,\pm1}^{0,-}\gg1$. Figure 2 shows the phase diagram for the existence of the $\nu=5,7$ QHE states with the same notations of Fig. 1. The agreement with the experimental results is remarkable: $\nu=5,7$ QHE states are observed and predicted for all samples of Ref. 2.

The exchange enhanced symmetric-antisymmetric gap, for $\nu=1$, is given as

$$\Delta_{\rm SAS}^x=2|T|+\frac{4e^2}{\varepsilon\ell_0}\int_0^\infty dq e^{-q^2/2}\int_{-1/2}^{1/2}dx \times\int_{-1/2}^{1/2}dx'\cos^2(\pi x)\cos^2(\pi x')e^{-q|d_l(x-x')-d|/\ell_0}, \tag{17}$$

where the last term for $d_l=0$ coincides with Eq. (10), for $\Delta=0$. We obtain that $(\Delta_{\rm SAS}^x-2|T|)/(e^2/\epsilon\ell_0)\approx0.34$, 0.33, and 0.31 for the samples of Ref. 2 with $d_l/d=0.83$, 0.78, and 0.73, respectively. The corresponding experimental val-

ues for $2|T|$ are 17.3, 8.1, and 3.9 K. Since $(e^2/\epsilon\ell_0) \simeq 200$ K, we see that $\Delta^x_{\rm SAS}$ is much larger than $\Delta_{\rm SAS} = 2|T|$.

IV. EFFECT OF CORRELATIONS ON THE COLLAPSE OF $\nu=1$ HALL GAP

In Sec. III it was demonstrated that our scenario of the $\nu=1$ Hall collapse within the HFA leads to the same results as in the experiment of Ref. 2 only when the approximation of zero thickness QW's, $d_l=0$, is used. For a more realistic model of the DQW's with finite thickness QW's, different results are obtained for two DQW samples used in Ref. 2. These HFA results clearly indicate that our model must be improved to take correlation effects into account. We include here the correlation effects, related with both the edge-state screening and quasiresonance screening in the inner part of the channel. The latter takes place when $2|T|$, $\Delta^x_{\rm SAS} \ll \hbar\omega_c$. First, we calculate explicitly the contributions to the Coulomb interaction $V^s(q_x;q_y,q_y';q_z,q_z')$ due to the screening by the edge states and the dominant contribution of the quasiresonance screening for the inner part of the channel, by extending the approach of Ref. 12 to the symmetric DQW structures. To simplify the notation, we will omit the indices of fixed $n=0$ and $\sigma=1$. Then $\varepsilon^{xc}_{k_x,\pm} \equiv \varepsilon^{xc}_{0,k_x,1,\pm}$, $k_r^- \equiv k^{0,-}_{r,1}$, $E_{k_x,\pm} \equiv E_{0,k_x,1,\pm}$, $\varepsilon_\pm(k_x) \equiv \varepsilon_{0,1,\pm}(k_x)$, and so on. Now it is convenient to present Eq. (5) in the form

$$\begin{aligned}\varepsilon^{xc}_{k_x,-} = &-\frac{1}{(2\pi)^5}\int_{-k_r^-}^{k_r^-} dk_x' \int_{-\infty}^{\infty}\cdots \\ &\times \int_{-\infty}^{\infty} dq_y dq_y' dq_z dq_z' V^s(k_-;q_y,q_y';q_z,q_z') \\ &\times \exp\{-[2k_-^2+q_y^2+(q_y')^2]\ell_0^2/4\} \\ &\times \exp[i(q_y+q_y')k_+\ell_0^2/2]\chi(q_z d_l)\chi(q_z' d_l) \\ &\times e^{i(q_z+q_z')(z_l+d/2)}\cos(q_z d/2)\cos(q_z' d/2), \end{aligned} \tag{18}$$

where we used the matrix elements $\langle X_{l,r}|e^{iq_z z}|X_{l,r}\rangle = e^{iq_z z_{l,r}}\chi(q_z d_l)$, with $\chi(a)=(2/a)\sin(a/2)/[1-(a/2\pi)^2]$.[13] The expression for $\varepsilon^{xc}_{k_x,+}$ is obtained by changing $\cos(q_z d/2)\cos(q_z' d/2)$ in Eq. (18) by $-\sin(q_z d/2)\sin(q_z' d/2)$.

The calculation of the Hall gap $G(v_g^H)$ proceeds essentially in the same way as in Ref. 12. Because the Fermi level E_F of the 2DES, pinned due to the edge effects at $E_F = E_{k_r^-,-}$, is closer to the bottom of the empty ($i=+$) LSL than to the bottom of the occupied ($i=-$) LSL, we have $G(v_g^H) = E_{0,+} - E_{k_r^-,-}$, where the energies given by Eqs. (3), (4), and (18) are calculated in the GLDA.

In order to determine $E_{0,+}$, we need to evaluate $\varepsilon^{xc}_{0,+}$. Since the edge-state screening does not affect $\varepsilon^{xc}_{0,+}$ for wide DQW channels, we look for the correlation effects coming only from the screening due to the inner part of the channel, neglecting here the edge effects. We consider, as in the experiments,[2,5] that $\hbar\omega_c \gg \Delta_{\rm SAS}$, and we assume also that $\hbar\omega_c \gg \Delta^{xc}_{\rm SAS}$, $\Delta^x_{\rm SAS}$. Then the dominant contribution (quasiresonance) to the screened potential in the interior part of the channel comes from the "bulk" screening related to virtual transitions between the two lowest LSL's. A straightforward calculation allows us to write the contribution to the Coulomb potential due to the screening effects of the inner part of the channel as

$$\begin{aligned}\Delta V^s_{\rm bulk}&(q_x;q_y,q_y';q_z,q_z') \\ &= -\frac{32\pi^2 e^4}{\epsilon^2\ell_0^2\Delta^{xc}_{\rm SAS}} \frac{\Pi(q_z;d_l,d)\Pi(q_z';d_l,d)}{q_x^2+q_y^2+q_z^2} \frac{\delta(q_y+q_y')}{q_x^2+q_y^2+(q_z')^2} \\ &\times e^{-(q_x^2+q_y^2)\ell_0^2/2}\left[1+\frac{4e^2}{\epsilon\ell_0^2\Delta^{xc}_{\rm SAS}} M_z(q_x,q_y;d_l,d)\right]^{-1}, \end{aligned} \tag{19}$$

where we have introduced the complex form factor

$$\Pi(q_z;d_l,d) = i\sin(q_z d/2)\chi(q_z d_l)e^{-iq_z(z_l+d/2)}, \tag{20}$$

and

$$M_z(q_x,q_y;d_l,d) = \frac{e^{-(q_x^2+q_y^2)\ell_0^2/2}}{\pi}\int_0^\infty dk_z \frac{|\Pi(k_z;d_l,d)|^2}{q_x^2+q_y^2+k_z^2}. \tag{21}$$

Substituting Eq. (19) into $\varepsilon^{xc}_{0,\pm}$, given by Eq. (18), we obtain that $\Delta V^s_{\rm bulk}$ makes a finite contribution to $\varepsilon^{xc}_{0,+}$ and exactly a null contribution to $\varepsilon^{xc}_{0,-}$. Then the symmetric-antisymmetric gap $\Delta^{xc}_{\rm SAS} = E_{0,+} - E_{0,-}$ renormalized by exchange and correlations can be written as

$$\Delta^{xc}_{\rm SAS} = \Delta^x_{\rm SAS} + \Delta\varepsilon^{xc}_{0,+}, \tag{22}$$

where $\Delta^x_{\rm SAS}$ is given by Eq. (17) and

$$\begin{aligned}\Delta\varepsilon^{xc}_{0,+} = &\frac{16e^4}{\pi\epsilon^2\ell_0^2\Delta^{xc}_{\rm SAS}}\int_0^\infty dq_x \\ &\times \int_0^\infty dq_y \frac{M_z^2(q_x,q_y;d_l,d)}{1+(4e^2/\epsilon\ell_0^2\Delta^{xc}_{\rm SAS})M_z(q_x,q_y;d_l,d)}. \end{aligned} \tag{23}$$

Equations (22) and (23) determine the self-consistent symmetric-antisymmetric gap, renormalized by exchange and correlations, so $\varepsilon^{xc}_{0,+}$. Indeed, from above it follows that

$$\varepsilon^{xc}_{0,+} = \varepsilon^x_{0,+} + \Delta\varepsilon^{xc}_{0,+}, \tag{24}$$

where

$$\varepsilon^x_{0,+} = -\frac{4e^2}{\pi\epsilon}\int_0^\infty dq_x \int_0^\infty dq_y M_z(q_x,q_y;d_l,d). \tag{25}$$

From Eqs. (23)–(25) we obtain that $\varepsilon^{xc}_{0,+} \to 0$ when formally $\Delta^{xc}_{\rm SAS} \to 0$. It means that the correlation effects, due to the quasiresonance screening, totally cancel the exchange term for the $i=+$ LSL.

In order to determine $E_{k_r^-,-}=E_F$, we follow the same steps of Ref. 12. Taking into account now only the edge-state screening, because the quasiresonance screening does not contribute to $E_{k_x,-}$, we arrive at the following expression for the screened Coulomb potential:

$$
\begin{aligned}
&V_-^s(q_x;q_y,q_y';q_z,q_z') \\
&\quad=\frac{4\pi}{\epsilon(q_x^2+q_y^2+q_z^2)}\Bigg(4\pi^2e^2\delta(q_y+q_y')\delta(q_z+q_z') \\
&\qquad-\frac{2\pi e^2 r(v_g)}{q_x^2+(q_y')^2+(q_z')^2}\chi(q_zd_l)\chi(q_z'd_l) \\
&\qquad\times\exp[-i(q_z+q_z')(z_l+d/2)]\cos(q_zd/2)\cos(q_z'd/2) \\
&\qquad\times\exp\{-[2q_x^2+q_y^2+(q_y')^2]\ell_0^2/4\} \\
&\qquad\times\exp[-i(q_y+q_y')(k_r^--q_x/2)\ell_0^2] \\
&\qquad\times[1+r(v_g)M(0,q_x;d_l,d)]^{-1}\Bigg),
\end{aligned}
\tag{26}
$$

where $v_g\equiv v_g^-$ is the group velocity of the edge states renormalized by exchange and correlations, the dimensionless parameter $r(v_g)=e^2/(\pi\hbar\epsilon v_g)$, and $M(0,q_x;d_l,d)$ is a special case of the matrix element

$$
\begin{aligned}
M(k_x-k_r^-,q_x;d_l,d)=\frac{2}{\pi}e^{-q_x^2\ell_0^2/2}\int_0^\infty dq_z \\
\times\int_0^\infty dq_y\frac{\exp(-q_y^2\ell_0^2/2)}{q_x^2+q_y^2+q_z^2}\chi^2(q_zd_l) \\
\times\cos^2(q_zd/2)\cos[q_y(k_x-k_r^-)\ell_0^2].
\end{aligned}
\tag{27}
$$

The group velocity of the edge states renormalized by exchange and correlations is given, as a function of v_g^H, by

$$
v_g=\frac{v_g^H}{2}\left\{1+\left[1+\frac{4e^2}{\pi\hbar\epsilon v_g^H}M(0,\delta/\ell_0;d_l,d)\right]^{1/2}\right\}, \tag{28}
$$

where $\delta\ll 1$ is a small cutting parameter that avoids the very weak Coulombic divergence as the wave vector tends to zero.[12] Our physically relevant results have a very weak dependence on δ. It can be estimated as $\delta\sim\max\{\ell_0/d_g;\ell_0/v_g\overline{\tau}\}$, where d_g is a typical distance to a remote screening gate and $\overline{\tau}$ is a typical lifetime for the edge states.

We use subscript in V_-^s to emphasize that we take into account in Eq. (26) only those terms in V^s that contribute to $E_{k_x,-}$. The first term in the curly brackets of Eq. (26) is the bare Coulomb interaction, which leads to the exchange contribution. The second term is related with strong screening by the edge states. The weak effect of the ''bulk'' nonresonance screening is neglected here. Furthermore, from Eqs. (18) and (26), it follows that the correlations due to the edge-state screening do not contribute to $\varepsilon_{k_x,+}^{xc}$. However, they strongly modify the dispersion $\varepsilon_{k_x,-}^{xc}$ of the occupied LSL in a wide region nearby the edge. We point out that the condition $W>\ell_0/\delta$ should be held for the assumed wide DQW channels; for typical $\ell_0\sim 10^{-6}$ cm and $\delta=10^{-3}$, it leads to $W>10^{-3}$ cm.

In the same way of the GLDA developed for a wide channel in the single-quantum well with zero thickness[12] (which has some similarity with the local-density approximation[15] and, especially, with the modified local-density approximation of Ref. 16), we point out that $E_{k_x,-}$ follows from the solution of the single-particle Schrödinger equation (for $i=-$) with the Hamiltonian $\hat{h}=\hat{h}^0+V_{xc}^-(y)$, where the self-consistent exchange-correlation potential $V_{xc}^-(y)=E_{y/\ell_0^2,-}-\varepsilon_-(y/\ell_0^2)$. Indeed, assuming that $V_{xc}^-(y)$ is smooth on the scale of ℓ_0 we find, neglecting small corrections, that the energy dispersion of $(i=-)$ LSL is given again by Eqs. (3), (4), (18), and (26)–(28). This confirms the self-consistency of the GLDA method to treat the present many-body problem. The assumed smoothness of the latter potential implies that v_g, given by Eq. (28), should satisfy the condition $v_g/\ell_0\ll\omega_c$, which can be rewritten as $v_g/(\hbar\omega_c/m^*)^{1/2}\ll 1$, where $(\hbar\omega_c/m^*)^{1/2}$ is the characteristic velocity.

Now we will study the effect of the correlations on the destruction of the $\nu=1$ Hall gap. From Eqs. (3), (4), (18), and (23)–(28), we obtain the Hall gap $G(v_g^H)$ as

$$
\begin{aligned}
G=2|T|-\frac{m^*\omega_c^2}{2\Omega^2}(v_g^H)^2-\frac{e^2}{\epsilon\ell_0}\int_0^\infty dq e^{-q^2/2}\int_{-1/2}^{1/2}dx \\
\times\int_{-1/2}^{1/2}dx'\cos^2(\pi x)\cos^2(\pi x') \\
\times(e^{-q(d_l/\ell_0)|x-x'|}-3e^{-q|d_l(x-x')-d|/\ell_0})+\Delta\varepsilon_{0,+}^{xc} \\
-\frac{e^2}{\pi\epsilon\ell_0}\int_0^\infty dt\frac{R(v_g^H)M^2(0,t_\delta/\ell_0;d_l,d)}{1+R(v_g^H)M(0,t_\delta/\ell_0;d_l,d)},
\end{aligned}
\tag{29}
$$

where by $R(v_g^H)$ we denote the function of v_g^H, which follows from $r(v_g)$, after v_g is expressed through v_g^H according to Eq. (28); $t_\delta=\sqrt{t^2+\delta^2}$. Here $\Delta\varepsilon_{0,+}^{xc}$ is determined by Eq. (23) and represents an upward shift of the $i=+$ LSL due to the correlations, caused by the quasiresonance bulk screening; i.e., these correlations contribute to increase the $\nu=1$ Hall gap. The last term in the right-hand side of Eq. (29) represents the contribution due to correlations induced by the edge-state screening. These correlations tend to destroy the $\nu=1$ Hall gap. Notice that their contribution tends to zero in the formal limit $v_g\to\infty$. A finite positive value of G means that $\nu=1$ QHE regime holds while the Hall gap collapses if $G\leqslant 0$. The HFA result for G is given by Eq. (29) when the last two terms are omitted.

We define $G_a(v_g^H)=G/|T|$ the dimensionless activation gap renormalized by exchange and correlations. In the absence of many-body interactions, the maximum value of $G_a=1$. So the activation gap is enhanced when $G_a>1$. No-

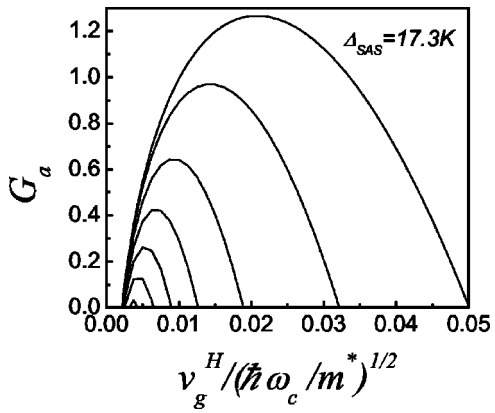

FIG. 3. Activation gap $G_a = G/(|T|)$ as a function of $v_g^H = v_{g0,1}^{-,H}$ for $\nu = 1$ in the DQW sample with $d_b = 28$ Å, $\Delta_{\rm SAS} = 2|T| = 17.3$ K, and the electron density $n_s = 4.2\times 10^{11}$ cm^{-2}. (Ref. 2). Here exchange and correlation effects are taken into account as well as a finite $d_l/d = 0.83$. From top to bottom G_a is shown for $\omega_c/\Omega = 7$, 10, 15, 20, 25, 30, and 35, respectively.

tice that for the usual activation gap[5] Δ_{ac}, determined from the resistivity $\rho_{xx} \propto \exp(-\Delta_{ac}/2k_B\,{\rm T})$, we have that $\Delta_{ac} = 2G$.

In Fig. 3 we show G_a, calculated from Eq. (29), as a function of v_g^H for $\nu = 1$, using the parameters of the DQW sample of Ref. 2 with $d_b = 28$ Å, $d_l/d = 0.83$, $2|T| = \Delta_{\rm SAS} = 17.3$ K, and the electron density $n_s = 4.2\times 10^{11}$ cm^{-2}. The curves correspond, from top to bottom, to $\omega_c/\Omega = 7$, 10, 15, 20, 25, 30, and 35, respectively; $\delta = 10^{-3}$. We observe that, for these values, the Hall gap is positive for $\omega_c/\Omega \leqslant 35$. However, there is a collapse for $\omega_c/\Omega > 35$. Notice that here $\omega_c = 4.54\times 10^{13}$ s^{-1} and the curves in Fig. 3 for $\omega_c/\Omega = 10$ and 30 correspond to $\Omega \approx 4.5\times 10^{12}$ s^{-1} and 1.5×10^{12} s^{-1}, respectively. As a consequence, we obtain that in this sample the $\nu = 1$ QHE state exists (more exactly, it is highly probable), which is in agreement with experiment.[2]

In Fig. 4, G_a is plotted as a function of v_g^H for $\nu = 1$ and another sample studied in Ref. 2 with $d_b = 40$ Å, $d_l/d = 0.78$, $2|T| = 8.1$ K, and $n_s = 3.8\times 10^{11}$ cm^{-2}. The curves correspond, from top to bottom, to $\omega_c/\Omega = 9$, 10, 15, 20, 25, and 30, respectively. From Fig. 4 it is seen that the $\nu = 1$ Hall gap is collapsed for $\omega_c/\Omega \geqslant 10$, which corresponds

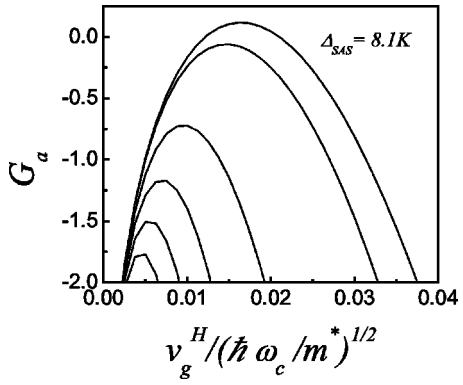

FIG. 4. From top to bottom, the curves correspond to $\omega_c/\Omega = 9$, 10, 15, 20, 25, and 30, respectively.

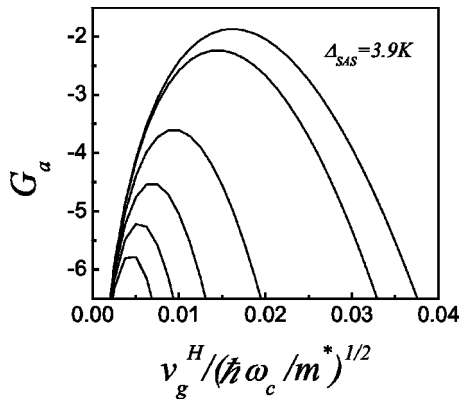

FIG. 5. Same as in Fig. 4 for the sample of Ref. 2 with $d_b = 51$ Å, $d_l/d = 0.73$, $2|T| = 3.9$ K, and $n_s = 3.9\times 10^{11}$ cm^{-2}.

to $\Omega \leqslant 4.11\times 10^{12}$ s^{-1}, since here ω_c is about 10% smaller than that in Fig. 3. So for this DQW sample, in agreement with the experiment,[2] we obtain that the $\nu = 1$ QHE cannot exist for rather realistic $\Omega \leqslant 4.11\times 10^{12}$ s^{-1}.

In Fig. 5 we present G_a as a function of v_g^H for $\nu = 1$ for the third sample of Ref. 2 with $d_b = 51$ Å, $d_l/d = 0.73$, $2|T| = 3.9$ K, and $n_s = 3.9\times 10^{11}$ cm^{-2}. In Fig. 5 we see that the $\nu = 1$ Hall gap is collapsed for $\omega_c/\Omega \gtrsim 10$. As now ω_c is close to that in Fig. 4, the curves in Fig. 5 correspond approximately to the same Ω as those curves in Fig. 4. We speculate that for this sample the above estimation $\Omega \leqslant 4.11\times 10^{12}$ s^{-1} is realistic too. So in agreement with the experiment,[2] for the DQW sample with $d_b = 51$ Å we obtain that the $\nu = 1$ QHE cannot exist. In summary, our model predicts, when both exchange and correlations are taken into account along with the finite d_l, the collapse of the $\nu = 1$ Hall gap in the case of the samples with $d_b = 40$ Å and $d_b = 51$ Å of Ref. 2.

The experimental results of Ref. 2 were obtained in the DQW samples with rather large tunneling splitting $\Delta_{\rm SAS} = 2|T| \gtrsim 4$ K. Now we compare our theoretical results with the experimental data for two samples of Ref. 5 with much smaller tunneling splitting $\Delta_{\rm SAS} \sim 0.5$ K. Both samples have $d_l = d_r = 180$ Å . For one sample, which we call A ($d_b = 31$ Å, $n_s = 1.26\times 10^{11}$ cm^{-2}, $\Delta_{\rm SAS} = 0.5$ K), a strong QHE state was found, while in the other sample B ($d_b = 40$ Å, $n_s = 1.45\times 10^{11}$ cm^{-2}, $\Delta_{\rm SAS} \approx 0.2$ K) the $\nu = 1$ QHE state is missing.

In Fig. 6, G_a, as a function of v_g^H, is depicted, using Eq. (29), for the $\nu = 1$ QHE state and for the parameters of sample A ($d_l/d = 0.853$, $d/\ell_0 = 1.88$, $r_0 = 1.146$, $B = 5.20$ T, $\hbar\omega_c = 103.7$ K). The solid, dashed, and dotted curves correspond to $\omega_c/\Omega = 3.7$, 3.9, and 4.3, and the confining frequency $\Omega \approx 3.65\times 10^{12}$ s^{-1}, 3.48×10^{12} s^{-1}, and 3.14×10^{12} s^{-1}, respectively; $\delta = 10^{-4}$. Notice that these values of Ω are in resonable agreement with the above estimation, for the samples of Ref. 2, of the maximum value of Ω ($\leqslant 4.11\times 10^{12}$ s^{-1}). Our result indicates that the $\nu = 1$ Hall gap is positive for $\omega_c/\Omega \leqslant 4.8$ and collapses only if $\omega_c/\Omega \geqslant 4.9$, which is in a good agreement with the observation[5] of the $\nu = 1$ QHE in sample A. In addition, from the maximum of G_a for the solid curve in Fig. 6 it follows

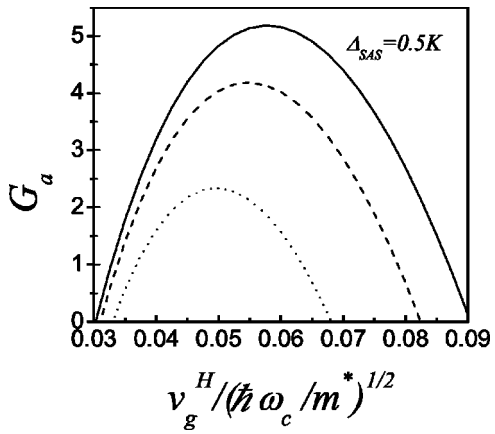

FIG. 6. Activation gap for the $\nu=1$ QHE in the DQW sample with parameters $d_b=31$ Å, $2|T|=0.5$ K, $n_s=1.26\times10^{11}$ cm^{-2} of Ref. 5. The solid, dashed, and dotted curves are obtained for $\omega_c/\Omega=3.7$, 3.9, and 4.3, respectively.

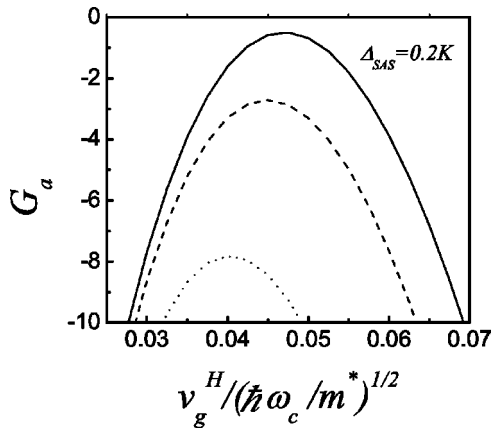

FIG. 7. Same as Fig 6 for the sample of Ref. 5 with $d_b=40$ Å, $2|T|\approx0.2$ K, $n_s=1.45\times10^{11}$ cm^{-2}. The solid, dashed, and dotted curves are for $\omega_c/\Omega=4.3$, 4.5, and 5.0, respectively, for the same values of Ω as in Fig. 6. In agreement with the experiment,[5] in this sample the $\nu=1$ Hall gap can be more easily destroyed, as for all the curves $G_a<0$, than in the sample of Fig. 6.

that $\Delta_{ac}=2G\approx10|T|=2.5$ K, which is of the same order as the experimental value $\Delta_{ac}\approx8.7$ K obtained for sample A in Ref. 5, without in-plane magnetic field.

Figure 7 exhibits our results for the parameters of sample B ($d_l/d=0.818$, $d/\ell_0=2.10$, $r_0=1.068$, $B=5.98$ T, $\hbar\omega_c=119.3$ K). The solid, dashed, and dotted curves correspond to $\omega_c/\Omega=4.3$, 4.5, and 5.0, respectively, i.e., for the same confining frequencies Ω as in Fig. 6; $\delta=10^{-4}$. Figure 7 shows that the Hall gap collapses when $\Omega\leqslant3.7\times10^{12}$ s^{-1}. This result is in a good agreement with the observation[5] of the $\nu=1$ Hall gap collapse in the sample B. We also observe that because $G_a<0$ for all curves in Fig. 7 the Hall gap can be more easily destroyed in sample B than in sample A in agreement with the experiment.[5]

V. CONCLUSIONS

In this work, we have studied exchange-correlation effects in odd integer QHE states in the DQW structures. First, we have shown that the combined effect of the lateral confinement and the exchange interaction can lead to collapse of odd integer Hall gaps, for $\nu=1, 3, 5, 7$. In particular, our model of zero thickness of the QW's predicts all observations of Ref. 2 for $\nu=1, 3, 5, 7$ QHE states except for the collapse of the $\nu=3$ Hall gap for the DQW sample with $d_b=51$ Å . However, for a more realistic model of the DQW structures ($d_l\neq0$), but still within the HFA, we have found that the $\nu=1$ Hall gap exists for all three samples of (Ref. 2). Since the gap is observed only for the sample with $d_b=28$ Å, we believe that the correlation effects would not be discarded in more realistic model of odd integer Hall gaps.

This is indeed the case because we have explained all pertinent to the $\nu=1$ Hall gap experimental results[2] after taking both exchange and correlations into account along with the $d_l\neq0$ model. It appears that the main correlations here result from the strong edge states screening.[12,16] These correlations tend to destroy the $\nu=1$ QHE state in the DQW structures. However, the correlations due to the quasiresonance bulk screening (which is present for the DQW samples of Ref. 2 because $\hbar\omega_c\gg\max\{\Delta_{\rm SAS},\Delta_{\rm SAS}^{xc}\}$), even much smaller than the former correlations, tend to recover the $\nu=1$ QHE state in the DQW structures. We have shown, in agreement with the experiment,[2] that for the realistic DQW model, with actual d_l/d, the exchange-correlation effects (i) destroy the $\nu=1$ Hall gaps for the samples with $d_b=40$ Å and $d_b=51$ Å; however, (ii) the $\nu=1$ Hall gap for the DQW sample with $d_b=28$ Å can be present.

We have also compared the results of our calculation for the $\nu=1$ Hall gap in the samples of Ref. 5 pertinent with the experimental results and have found a reasonable agreement.

ACKNOWLEDGMENTS

This work was supported in part by a grant from Fundação de Amparo à Pesquisa do Estado de São Paulo (FAPESP). The authors are grateful to Conselho Nacional de Desenvolvimento Cientifico e Technológico (CNPq) for financial support for this research.

[1] For a recent review of the QHE in DQW's, see the chapters by J. P. Eisenstein, and by S. M. Girvin and A. H. MacDonald in *Perspectives in Quantum Hall Effects*, edited by S. Das Sarma and A. Pinczuk (Wiley, New York, 1997); see also S.M. Girvin, cond-mat/0108181.

[2] G.S. Boebinger, H.W. Jiang, L.N. Pfeiffer, and K.W. West, Phys. Rev. Lett. **64**, 1793 (1990).

[3] Y. W Suen, J. Jo, M.B. Santos, L.W. Engel, S.W. Hwang, and M. Shayegan, Phys. Rev. B **44**, 5947 (1991).

[4] G.S. Boebinger, L.N. Pfeiffer, and K.W. West, Phys. Rev. B **45**,

11 391 (1992).
[5] S.Q. Murphy, J.P. Eisenstein, G.S. Boebinger, L.N. Pfeiffer, and K.W. West, Phys. Rev. Lett. **72**, 728 (1994).
[6] A.H. MacDonald, P.M. Platzman, and G.S. Boebinger, Phys. Rev. Lett. **65**, 775 (1990).
[7] L. Brey, Phys. Rev. Lett. **65**, 903 (1990); Phys. Rev. B **47**, 4585 (1993).
[8] S. He, S. Das Sarma, and X.C. Xie, Phys. Rev. B **47**, 4394 (1993).
[9] I.B. Spielman, J.P. Eisenstein, L.N. Pfeiffer, and K.W. West, Phys. Rev. Lett. **84**, 5808 (2000).
[10] J. Schliemann, S.M. Girvin, and A.H. MacDonald, Phys. Rev. Lett. **86**, 1849 (2001).
[11] B.I. Halperin, Phys. Rev. B **25**, 2185 (1982).
[12] O.G. Balev and Nelson Studart, Phys. Rev. B **64**, 115309 (2001).
[13] F.T. Vasko, O.G. Balev, and P. Vasilopoulos, Phys. Rev. B **47**, 16 433 (1993).
[14] O.G. Balev and P. Vasilopoulos, Phys. Rev. B **59**, 2063 (1999).
[15] T. Ando, A.B. Fowler, and F. Stern, Rev. Mod. Phys. **54**, 437 (1982).
[16] O.G. Balev and P. Vasilopoulos, Phys. Rev. B **56**, 6748 (1997).